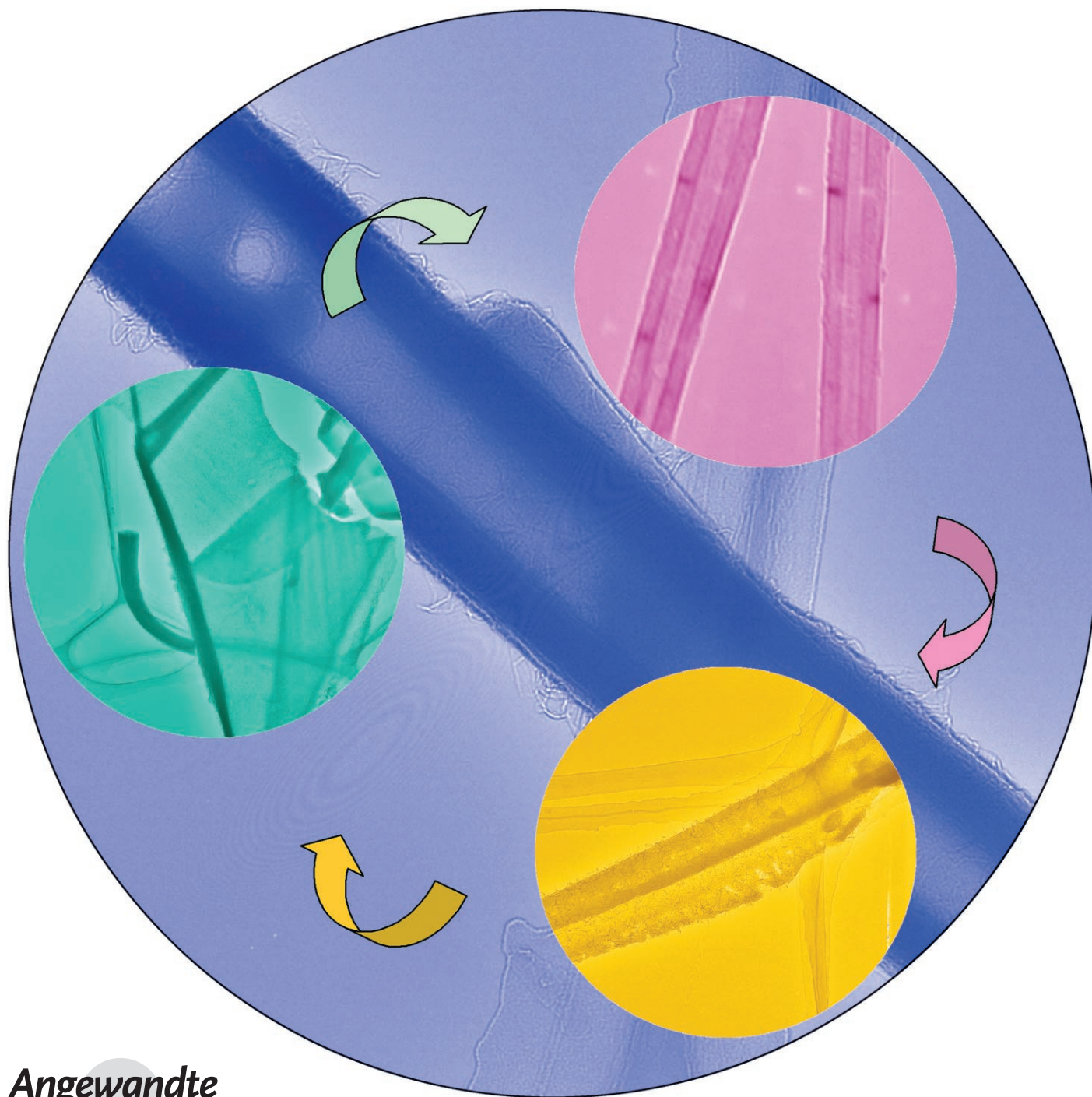


Formation of Crystalline SrAl_2O_4 Nanotubes by a Roll-Up and Post-Annealing Approach**

Changhui Ye,* Yoshio Bando, Guozhen Shen, and Dmitri Golberg



Soon after the identification of carbon nanotubes,^[1] it was demonstrated that many layered inorganic compounds could be prepared in tubular morphologies.^[2] The formation of inorganic nanotubes was suggested to occur by a curving and seaming process. Later, artificial lamellar structures were prepared in solution, from which nanotubes (or nanoscrolls) could be formed after heat treatment.^[3] The thermally driven roll-up of thin layers into scrolls as a result of lattice expansion mismatch was also reported.^[4] Such a process occurs when a two-layer thin film of Si/SiGe is heated: the film rolls up to form nanoscrolls, owing to the asymmetric strain on its two sides.^[4b,d]

The bending and roll-up of a thin layer to form tubular nanoscrolls is a thermally driven process. A layer with dangling bonds at its periphery is unstable. The decrease in the number of dangling bonds and reduction in the area of the active solid–vapor or solid–liquid interface that occur upon bending compensate the energy barrier associated with the strain of bending.^[5] Thus, the formation of seamless nanotubes or nanoscrolls can be energetically favorable. As a result of bending, defects are commonly generated within a structure to allow strain release, which is beneficial for the overall stabilization of the tubular structure.

From a kinetic point of view, the rolling of the lamellar structure may be initiated by a stress of either a structural or an electrical nature caused by the asymmetry of the layer. Recently, Mallouk and co-workers demonstrated that the free-energy difference between the coiled and uncoiled forms of an exfoliated colloid was rather small; therefore, the occurrence of rolled-up nanoscrolls or unrolled layers depends on the chemical environment (such as the ionic strength and pH).^[3d,e]

To date, there has been much theoretical and experimental work relating to the synthesis of inorganic nanotubes from layered or artificial lamellar structures and their mechanisms of formation. However, direct evidence of the bending, seaming, and roll-up processes is still lacking.^[1–5] In addition, controversial arguments have recently arisen; for example, Kukovec et al. have questioned the roll-up mechanism for the formation of nanotubes from lamellar structures.^[6] In fact, these authors found nanoloop intermediates and proposed an oriented-attachment mechanism for the formation of nanotubes. This hypothesis accounts for the fact that a smaller driving force is involved in the formation of nanotubes than that theoretically predicted for the roll-up of a layer. In contrast, our present results explicitly demonstrate that the

roll-up of a whole layer has indeed taken place and has contributed to nanoscroll formation.

Strontium aluminate (SrAl_2O_4) is one of the most studied and most efficient host materials for long-lasting phosphorescence.^[7] The low-temperature phase of SrAl_2O_4 adopts a monoclinic structure (space group $P2_1$, $a = 8.447$, $b = 8.816$, $c = 5.163$ Å, and $\beta = 93.42^\circ$) that consists of a three-dimensional network of corner-sharing $\{\text{AlO}_4\}$ tetrahedra containing connected open channels, in which the Sr^{2+} ions are located.^[7b] Rare-earth ions with the same valence and a similar radius to Sr^{2+} (1.21 Å), such as Eu^{2+} (1.20 Å), can be readily substituted for Sr^{2+} with minor (if any) local distortion of the crystal lattice.^[7b] This property makes SrAl_2O_4 an ideal host material for long-lasting phosphorescence. The synthesis and optical properties of SrAl_2O_4 , in bulk form, or as films or nanoparticles, have been extensively explored during the past decades.^[8] However, the production of one-dimensional aluminate nanomaterials has lingered far behind. To date, only one paper on the synthesis of SrAl_2O_4 nanorods has been published; however, neither the details of the synthesis nor a complete structural characterization of the nanorods were provided.^[9] Nanotubes of alkaline-earth-metal aluminates have not yet been observed.

Herein, we report the rational synthesis of crystalline SrAl_2O_4 nanotubes by a roll-up and post-annealing route under hydrothermal conditions. In contrast to the synthesis of BaAl_2O_4 , a mixture of cetyltrimethylammonium bromide (CTAB)/*n*-butanol/water, rather than CTAB/water, was used as the reaction medium, allowing a high loading of ionic reactants and a more efficient modulation of morphology.^[10] Urea was used as a slow-release pH-adjusting agent. The products obtained after heating at 120 °C for 16 h possessed a whisker-like morphology, as shown in a scanning electron microscopy (SEM) image (Figure 1a).

To further investigate the product morphology and structure, transmission electron microscopy (TEM) and high-resolution (HR) TEM were employed. As shown in the TEM image of Figure 1b, the products have a tubular morphology. The selected area electron diffraction (SAED) pattern shown in the inset reveals that the nanotubes are amorphous. It is apparent that the nanotube diameter is not uniform throughout the whole length, which will be discussed below.

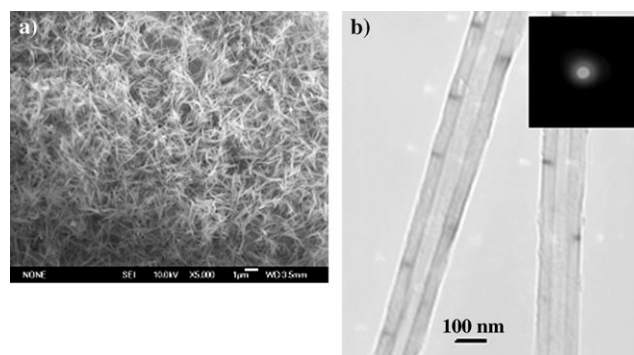


Figure 1. a) SEM image of the SrAl_2O_4 product synthesized at 120 °C; scale bar = 1 μm. b) TEM image of two as-synthesized SrAl_2O_4 nanotubes; corresponding SAED pattern in inset.

[*] Dr. C. Ye, Prof. Y. Bando, Dr. G. Shen, Prof. D. Golberg
Nanoscale Materials Center
National Institute for Materials Science
Namiki 1-1, Tsukuba, Ibaraki 305-0044 (Japan)
Fax: (+81) 29-851-6280
E-mail: Ye.Changhui@nims.go.jp

[**] This work was supported by the Japan Society for the Promotion of Science (JSPS), in the form of a fellowship tenable at the National Institute for Materials Science, Tsukuba, Japan (C.Y.).

Supporting information for this article is available on the WWW under <http://www.angewandte.org> or from the author.

Note that the nanotubes were not induced by the sonication during the preparation of the TEM samples, because nanotubes were observed in the as-synthesized products (see Supporting Information).

In order to obtain well-crystallized SrAl_2O_4 nanotubes, we annealed the product at 1300°C for 4 h. From the TEM image of an annealed nanotube shown in Figure 2a, it is clear that

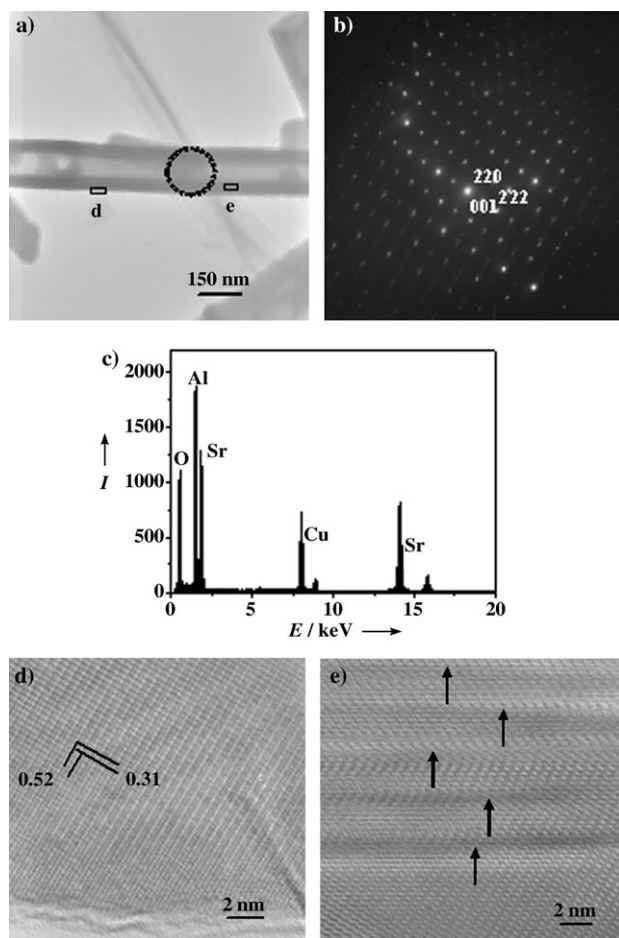


Figure 2. a) TEM image of a post-annealed SrAl_2O_4 nanotube. b) SAED pattern of the area circled in (a), recorded along the $[1\bar{1}0]$ zone axis. c) EDX spectrum of the nanotube. d) and e) HRTEM images corresponding to the marked regions in (a); in (d), lattice spacings discussed in text are indicated; the arrows in (e) point out stacking faults and antiphase boundaries.

the tubular morphology is preserved upon high-temperature annealing. An SAED pattern taken along the $[1\bar{1}0]$ zone axis demonstrates the single-crystalline nature of the nanotube (Figure 2b). The slight streaking of the diffraction spots indicates that planar defects are present within the nanotube. Energy dispersive X-ray (EDX) spectroscopy indicates that the nanotube is composed of strontium, aluminum, and oxygen in an atomic ratio that agrees with the stoichiometric formula SrAl_2O_4 (Figure 2c; the copper signal is due to the carbon-coated copper grid used as a sample holder). An HRTEM image shows the lattice fringes corresponding to the $\{001\}$ and $\{220\}$ planes, which have spacings of approximately

0.52 and 0.31 nm, respectively (Figure 2d). The nanotube walls are not perfect single crystals; as indicated by the arrows in Figure 2e, stacking faults and antiphase boundaries are present, consistent with the streaking observed in the SAED pattern. Note that antiphase boundary defects are common in SrAl_2O_4 and related materials.^[11]

The nanotube growth mechanism was investigated by systematically studying the evolution of the product morphology during the hydrothermal process. When the heating time is shorter than 2 h at 120°C , no solid product is produced, because an incubation period is necessary prior to nucleation. When the heating time is extended to 4–8 h, nanoparticles and nanoplatelets appear (see Supporting Information). A further extension of the heating time to 10 h results in the appearance of nanoscrolls. In Figure 3, both

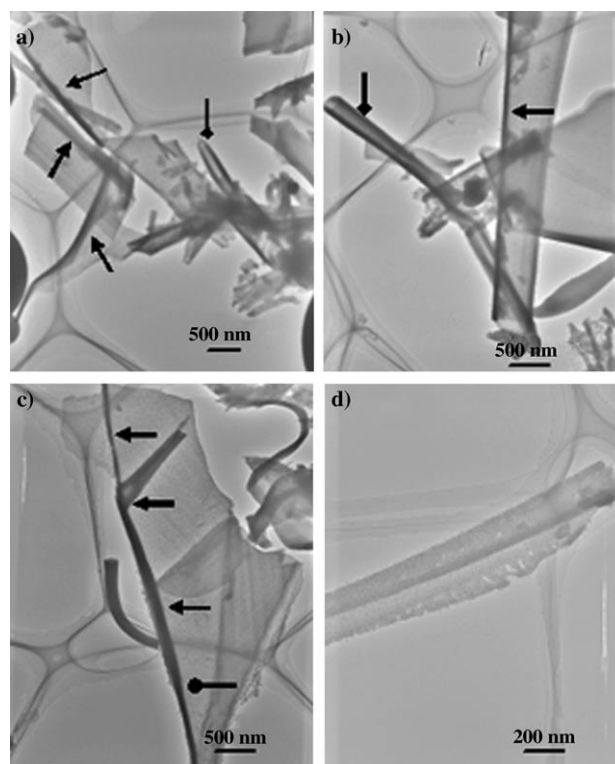


Figure 3. TEM images of the roll-up of SrAl_2O_4 layers to form nanoscrolls during hydrothermal synthesis at 120°C ; the arrows in (a)–(c) point out structural features described in text.

nanoscrolls and nanoplatelets can be seen; the triangle arrowheads indicate the roll-up of nanoplatelets, and the diamond arrowheads indicate the roll-up of nanoscrolls. Note that the nanoplatelets are flexible enough to bend, but are rigid enough to bear the bending stress. It is rare to find a broken platelet, such as the one indicated by the triangle arrowhead with the thick tail in Figure 3c. From the TEM images, it is clear that the nanoplatelets are not uniform in shape; therefore, the diameter of the rolled-up nanoscrolls is not axially uniform, as indicated by the round arrowhead in Figure 3c. In Figure 3d, a nanoscroll near the end of the roll-up process is shown; it is again apparent that the diameter of the nanoscroll is not uniform throughout its length.

As discussed above, the as-synthesized nanoscrolls are amorphous prior to high-temperature annealing, as is characteristic for alkaline-earth-metal aluminates. After annealing at 1300 °C for 4 h, the nanoscrolls are fully transformed into crystalline nanotubes of monoclinic SrAl_2O_4 . Nanoscrolls and nanotubes can be clearly differentiated: nanoscrolls are rolled up from a single sheet, whereas the original layered structure is lost in nanotubes, as a result of an atomic rearrangement. When the amorphous samples are annealed, $\{\text{AlO}_4\}$ tetrahedra are formed through a dehydration process. During the rearrangement of the atoms within the layers, the $\{\text{AlO}_4\}$ units may change their original positions and orientations to fit the resultant crystal symmetry of the monoclinic phase. Long-range ordering is an energy-consuming process; therefore, by virtue of the strain present in the nanoscrolls, crystals exhibiting stacking faults and antiphase boundaries are formed.

As stated above, the bending and roll-up of layers are thermally driven processes; that is, thermal energy is needed to overcome the potential-energy barrier associated with the induced strain. According to Yada et al.,^[3c] Sun and Li,^[3j] and Xiong et al.,^[3i] hydrothermal reaction at higher temperatures favors the formation of solid rods. Because of the larger thermal energy input, the roll-up process begins at a smaller starting diameter, leaving a smaller hollow space in the nanoscroll. A small hollow space could be easily annealed out to form solid rods, whereas a large hollow space would be preserved to form hollow tubes upon annealing, as observed.^[3c,i,j]

We carried out hydrothermal reactions at 180 °C for 10–48 h (without post-annealing) and invariably obtained solid nanorods. As shown in Figure 4, the nanorods are generally smaller than 50 nm in diameter, much thinner than the nanotubes. Some nanorods are bundled. Our results agree well with those reported previously.^[3c,i,j]

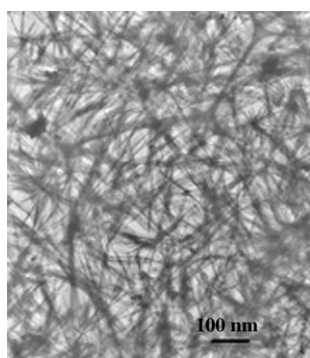


Figure 4. TEM image of SrAl_2O_4 nanorods synthesized at 180 °C.

In conclusion, single-crystalline SrAl_2O_4 nanotubes have been synthesized by a roll-up and post-annealing approach. We have found evidence for a roll-up mechanism driven by thermal energy, which compensates the surface energy. We have also found that the use of higher temperatures and pressures during the hydrothermal treatment favors the formation of solid nanorods over nanotubes. This facile preparation method could be extended to other materials,

such as titanates and zirconates. The single-crystalline SrAl_2O_4 nanotubes may find important applications in after-glow and luminescence.

Experimental Section

All chemicals were used as received without further purification.

Growth of SrAl_2O_4 nanotubes: $\text{Al}(\text{NO}_3)_3 \cdot 9\text{H}_2\text{O}$ (4 mmol), $\text{Sr}(\text{NO}_3)_2$ (2 mmol), urea (0.01 mol), *n*-butanol (0.1 mol), and CTAB (2 mmol) were dissolved in deionized water (50 mL) and stirred magnetically for 2 h. Then, the solution was poured into two teflon-lined autoclaves of 40-mL capacity. The two solutions were treated under different experimental conditions, and were heated at temperatures in the range 100–180 °C for 30 min to 48 h. Post-annealing was carried out at 1200–1350 °C for 4 h in air.

Characterization: SEM images were recorded for as-synthesized samples on a JEOL JSM-6700F microscope. TEM and HRTEM images, and EDX spectra were recorded on a JEOL JEM-3000F microscope at an acceleration voltage of 300 kV. Samples were sonicated for several minutes in ethanol, and then several drops of the sample solutions were dripped onto carbon-coated copper grids.

Received: April 4, 2006

Published online: July 3, 2006

Keywords: aluminum · hydrothermal synthesis · nanostructures · nanotubes · strontium

- [1] S. Iijima, *Nature* **1991**, 354, 56.
- [2] a) R. Tenne, L. Margulis, M. Genut, G. Hodes, *Nature* **1992**, 360, 444; b) Y. Feldman, E. Wasserman, D. J. Srolovitz, R. Tenne, *Science* **1995**, 267, 222; c) N. G. Chopra, R. J. Luyken, K. Cherrey, V. H. Crespi, M. L. Cohen, S. G. Louie, A. Zettl, *Science* **1995**, 269, 966; d) P. M. Ajayan, O. Stephan, P. Redlich, C. Colliex, *Nature* **1995**, 375, 564; e) Y. R. Hachohen, E. Grunbaum, R. Tenne, J. Sloan, J. L. Hutchison, *Nature* **1998**, 395, 336; f) J. A. Hollingsworth, D. M. Poojary, A. Clearfield, W. E. Buhro, *J. Am. Chem. Soc.* **2000**, 122, 3562; g) M. Nath, C. N. R. Rao, *J. Am. Chem. Soc.* **2001**, 123, 4841; h) Y. Li, J. Wang, Z. Deng, Y. Wu, X. Sun, D. Yu, P. Yang, *J. Am. Chem. Soc.* **2001**, 123, 9904; i) C. Ye, G. Meng, Z. Jiang, Y. Wang, G. Wang, L. Zhang, *J. Am. Chem. Soc.* **2002**, 124, 15180; j) M. Brorson, T. W. Hansen, C. J. H. Jacobsen, *J. Am. Chem. Soc.* **2002**, 124, 11582; k) M. Nath, C. N. R. Rao, *Angew. Chem.* **2002**, 114, 3601; *Angew. Chem. Int. Ed.* **2002**, 41, 3451; l) Y. R. Hachohen, R. Popovitz-Biro, E. Grunbaum, Y. Prior, R. Tenne, *Adv. Mater.* **2002**, 14, 1075; m) J. Chen, Z. Tao, S. Li, *Angew. Chem.* **2003**, 115, 2197; *Angew. Chem. Int. Ed.* **2003**, 42, 2147; n) J. Chen, Z. Tao, S. Li, X. Fan, S. Chou, *Adv. Mater.* **2003**, 15, 1379; o) S. Y. Hong, R. Popovitz-Biro, Y. Prior, R. Tenne, *J. Am. Chem. Soc.* **2003**, 125, 10470; p) U. K. Gautam, S. R. C. Vivekchand, A. Govindaraj, G. U. Kulkarni, N. R. Selvi, C. N. R. Rao, *J. Am. Chem. Soc.* **2005**, 127, 3658.
- [3] a) M. Remskar, Z. Skraba, F. Cleton, R. Sanjines, F. Levy, *Appl. Phys. Lett.* **1996**, 69, 351; b) R. Abe, K. Shinohara, A. Tanaka, M. Hara, J. N. Kondo, K. Domen, *Chem. Mater.* **1997**, 9, 2179; c) M. Yada, H. Hiyoshi, K. Ohe, M. Machida, T. Kijima, *Inorg. Chem.* **1997**, 36, 5565; d) G. B. Saupe, C. C. Waraksa, H. N. Kim, Y. Han, D. M. Kaschak, D. M. Skinner, T. E. Mallouk, *Chem. Mater.* **2000**, 12, 1556; e) R. E. Schaak, T. E. Mallouk, *Chem. Mater.* **2000**, 12, 3427; f) G. Du, Q. Chen, R. Che, Z. Yuan, L. Peng, *Appl. Phys. Lett.* **2001**, 79, 3702; g) Y. Li, X. Li, R. He, J. Zhu, Z. Deng, *J. Am. Chem. Soc.* **2002**, 124, 1411; h) M. Mo, J. Zeng, X. Liu, W. Yu, S. Zhang, Y. Qian, *Adv. Mater.* **2002**, 14, 1658; i) X. Sun, Y. Li, *Chem. Eur. J.* **2003**, 9, 2229; j) Y. Xiong, Y.

- Xie, Z. Li, X. Li, S. Gao, *Chem. Eur. J.* **2004**, *10*, 654; k) S. V. Krivovichev, V. Kahlenberg, R. Kaindl, E. Mersdorf, I. G. Tananaev, B. F. Myasoedov, *Angew. Chem.* **2005**, *117*, 1158; *Angew. Chem. Int. Ed.* **2005**, *44*, 1134; l) J. Hu, Y. Bando, J. Zhan, Z. Liu, D. Golberg, *Appl. Phys. Lett.* **2005**, *87*, 153112.
- [4] a) V. Y. Prinz, V. A. Seleznev, A. K. Gutakovsky, A. V. Chehofskiy, V. V. Preobrazhenskii, M. A. Putyato, T. A. Gavrilova, *Phys. E* **2000**, *6*, 828; b) Q. G. Schmidt, K. Eberl, *Nature* **2001**, *410*, 168; c) V. Y. Prinz, D. Grutzmacher, A. Beyer, C. David, B. Ketterer, E. Deckardt, *Nanotechnology* **2001**, *12*, 399; d) S. V. Golod, V. Y. Prinz, V. I. Mashanov, A. K. Gutakovsky, *Semicond. Sci. Technol.* **2001**, *16*, 181; e) Y. V. Nastaushchev, V. Y. Prinz, S. N. Svitashcheva, *Nanotechnology* **2005**, *16*, 908.
- [5] a) D. J. Srolovitz, S. A. Safran, M. Homyonfer, R. Tenne, *Phys. Rev. Lett.* **1995**, *74*, 1779; b) G. Seifert, T. Kohler, R. Tenne, *J. Phys. Chem. B* **2002**, *106*, 2497; c) S. Zhang, L. Peng, Q. Chen, G. Du, G. Dawson, W. Zhou, *Phys. Rev. Lett.* **2003**, *91*, 256103; d) F. Xu, J. Hu, Y. Bando, *J. Am. Chem. Soc.* **2005**, *127*, 16860.
- [6] A. Kukovecz, N. Hodos, E. Horvath, G. Radnocy, Z. Konya, I. Kiricsi, *J. Phys. Chem. B* **2005**, *109*, 17781.
- [7] a) T. Katsumata, S. Toyomane, A. Tonegawa, Y. Kanai, U. Kaneyama, K. Shakuno, R. Sakai, S. Komuro, T. Morikawa, *J. Cryst. Growth* **2002**, *237*, 361; b) F. Clabau, X. Rocquefelte, S. Jobic, P. Deniard, M. H. Whangbo, A. Garcia, T. Le Mercier, *Chem. Mater.* **2005**, *17*, 3904; c) Y. Liu, C. Xu, *J. Phys. Chem. B* **2003**, *107*, 3991; d) J. Holsa, T. Aitasalo, H. Jungner, M. Lastusaari, J. Niittytoski, G. Spano, *J. Alloys Compd.* **2004**, *374*, 56.
- [8] a) Z. Fu, S. Zhou, S. Zhang, *J. Phys. Chem. B* **2005**, *109*, 14396; b) P. Escibano, M. Marchal, M. L. Sanjuán, P. A. Gutiérrez, B. Julián, E. Cordocillo, *J. Solid State Chem.* **2005**, *178*, 1978; c) L. Wang, Y. Zhu, *J. Alloys Compd.* **2004**, *370*, 276; d) N. Honda, T. Suzuki, T. Yunogami, H. Suematsu, W. Jiang, K. Yatsui, *Jpn. J. Appl. Phys.* **2005**, *44*, 695.
- [9] Y. Lin, Z. Zhang, F. Zhang, Z. Tang, Q. Chen, *Mater. Chem. Phys.* **2000**, *65*, 103.
- [10] a) M. Husein, E. Rodil, J. Vera, *Langmuir* **2003**, *19*, 8467; b) M. Husein, E. Rodil, J. Vera, *Langmuir* **2006**, *22*, 2264.
- [11] M. L. Ruiz-González, J. M. González-Calbet, M. Vallet-Regí, E. Cordocillo, P. Escibano, J. B. Carda, M. Marchal, *J. Mater. Chem.* **2002**, *12*, 1128.